# 추계론적 유한 요소법을 이용한 동하중을 받는 비선형 구조물의 안전성 평가

# Nonlinear Structural Safety Assessment under Dynamic Excitation Using SFEM

허 정 원*
Huh, Jungwon

요 지

단기 동 하중(특히 지진하중)을 받는 비선형 강 프레임 구조물의 안전성을 평가하기 위하여 추계론적 유한요소 개념에 근거한 비선형 시간영역 신뢰성 해석 기법을 제안하였다. 제안된 알고리즘에서는 유한요소 공식화가 응답 표면법, 1차 신뢰성 방법, 그리고 반복 선형보간 기법의 개념들과 결합되어 지는데, 이것이 추계론적 유한요소 개념으로 귀결된다. 실제 지진하중의 시간이력이 구조물의 진동을 위해 사용되므로 사실적인 하중조건의 재현이 가능하다. 가상 응력에 기초한 유한요소 기법이 본 알고리즘의 효율성을 증대하기 위해 사용된다. 본 알고리즘은 지진하중 또는 임의의 단기 동적하중을 받는 유한요소 기법으로 표현되는 어떠한 선형 및 비선형 구조물과 관련된 위험도를 평가할 수 있는 잠재성을 가지고 있다. 수치예제를 통하여 알고리즘을 설명하였으며, 몬테카를로 시뮬레이션 기법을 사용하여 본 알고리즘을 검증하였다.

**핵심용어** : 추계론적 유한요소법, 지진하중, 시간이력, 주파수관련 특성, 가상응력 유한요소법, 응답표면법

## Abstract

To assess the safety of nonlinear steel frame structures subjected to short duration dynamic loadings, especially seismic loading, a nonlinear time domain reliability analysis procedure is proposed in the context of the stochastic finite element concept. In the proposed algorithm, the finite element formulation is combined with concepts of the response surface method, the first order reliability method, and the iterative linear interpolation scheme. This leads to the stochastic finite element concept. Actual earthquake loading time-histories are used to excite structures, enabling a realistic representation of the loading conditions. The assumed stress-based finite element formulation is used to increase its efficiency. The algorithm also has the potential to evaluate the risk associated with any linear or nonlinear structure that can be represented by a finite element algorithm subjected to seismic loading or any short duration dynamic loading. The algorithm is explained with help of an example and verified using the Monte Carlo simulation technique.

***Keywords*** : *stochastic finite element method, seismic loading, time-history, frequency content, assumed stress-based FEM, response surface method*

* 정회원 · 연세대학교 토목공학과, 박사후 전문연구원 (Post Doctoral)

• 이 논문에 대한 토론을 2000년 12월 31일까지 본 학회에 보내주시면 2001년 3월호에 그 결과를 게재하겠습니다.

## 1. Introduction

The safety of a structural system depends on the loads or the load combinations to which will be subjected during its lifetime and the load-carrying capacity (or resistance) of the structure or its components. The presence of uncertainties in the load and parameters related to load-carrying capacity is well known in the profession and the absolute assurance of the safety of a structural system is not possible. Therefore, in codified approaches, load and resistance factors are used to address the uncertainties, leading the reliability-based design. In spite of significant advances in analytical capabilities and design philosophies, the realistic safety assessment of structures under short duration dynamic loadings has yet to be addressed comprehensively. The subject of this paper is reliability assessment of such structures with realistic modeling of dynamic loadings and resistance-related parameters.

Most structures will show nonlinear behavior just before failure. Thus, in the estimation of failure probability, the nonlinear behavior of structures cannot be avoided. To evaluate the safety of complicated structures subjected to time-variant loadings in the presence of different sources of nonlinearity, a finite element method (FEM) -based formulation is desirable. In this way, different factors (support and connection conditions, geometric and material conditions, etc.) and the nonlinearity associated with them can be easily incorporated. It is also the first step in a conventional deterministic analysis. The use of FEM in the context of uncertainty leads to the concept of stochastic finite element method (SFEM).

Time-variant loadings, i.e., seismic and other short-duration loadings, cause a significant amount of damage to structures and are very unpredictable. Therefore, the incorporation of uncertainties in the time history analysis is very desirable for the reliability analysis of nonlinear structures subjected to seismic loadings. The class of Monte Carlo simulation method (MCS) can be used for this purpose. However, it may be too costly and cumbersome for the simulation of nonlinear time-history analysis of dynamic systems. The stochastic finite element method (SFEM) for static problems as proposed by Haldar and Gao[1] has been proved to be very elegant, economical, and accurate. Although, using this algorithm, the reliability can be estimated at every time increment of the acceleration of a seismic loading, it will be very difficult and be too time-consuming to apply the algorithm to the problem under consideration. The response surface method (RSM) has the potential to consider the uncertainty in the short duration dynamic load and resistance-related parameters without compromising the efficiency and accuracy to a great extent. It is the goal of this study to develop such a hybrid algorithm by combining the RSM, the FEM, and the first order reliability method (FORM).

## 2. Assumed Stress-based FEM for Dynamic Analysis

The efficiency of the deterministic finite element method is important in the implementation of SFEM since the analysis is based on tracking the uncertainty propagating through the steps of deterministic analysis. It has been reported in the literature[2),3),4)] that the assumed stress-based finite element method has many advantages over the displacement-based method, particularly for nonlinear analysis of large deformation problems. In the assumed stress-based finite element method, the tangent stiffness can be expressed in explicit form, the stresses of an element can be obtained directly, fewer elements are required to describe a large deformation configuration, and integration is not required to obtain the tangent stiffness.

Different sources of nonlinearity can be incorporated without losing the basic simplicity. It is very accurate and efficient in analyzing nonlinear responses. Some of its essential features in the context of dynamic problems are discussed in the following sections.

### 2.1 Dynamic Governing Equation

The nonlinear dynamic equilibrium equation can be expressed at time $t+\Delta t$ as

$$\mathbf{M}\ {}^{t+\Delta t}\ddot{\mathbf{D}}^{(k)} + {}^{t}\mathbf{C}\ {}^{t+\Delta t}\dot{\mathbf{D}}^{(k)} + {}^{t}\mathbf{K}^{(k)}\ {}^{t+\Delta t}\Delta\mathbf{D}^{(k)} = {}^{t+\Delta t}\mathbf{F}^{(k)} - {}^{t+\Delta t}\mathbf{R}^{(k-1)} - \mathbf{M}\ {}^{t+\Delta t}\ddot{\mathbf{D}}_{g}^{(k)} \qquad (1)$$

where ${}^{t}\mathbf{K}^{(k)}$ is the global tangent stiffness matrix of the $k^{th}$ iteration at time $t$, ${}^{t+\Delta t}\Delta\mathbf{D}^{(k)}$ is the incremental displacement vector of the $k^{th}$ iteration at time $t+\Delta t$, ${}^{t+\Delta t}\mathbf{F}^{(k)}$ is the external load vector of the $k^{th}$ iteration at time $t+\Delta t$, ${}^{t+\Delta t}\mathbf{R}^{(k-1)}$ is the internal force vector of the $(k-1)^{th}$ iteration at time $t+\Delta t$, $\mathbf{M}$ is the mass matrix, ${}^{t}\mathbf{C}$ is the viscous damping coefficient matrix at time $t$, and ${}^{t+\Delta t}\ddot{\mathbf{D}}_{g}^{(k)}$ is the seismic ground acceleration vector of the $k^{th}$ iteration at time $t+\Delta t$.

The procedures to estimate all these parameter matrices are discussed briefly here. First, for the mass matrix $\mathbf{M}$, either a lumped mass matrix or consistent mass matrix can be used. Second, using the assumed stress method, the tangent stiffness matrix and the internal force vector for each beam-column element at the $k^{th}$ iteration at a given time $t$ can be expressed explicitly depending on the existence of the material nonlinearity. They are not provided in here since they are widely available in the literature[2),3),4)]. Finally, the damping matrix ${}^{t}\mathbf{C}$ in Eq. (1) is considered to be viscous in this study. Using the equivalent viscous damping varying between 0.1% to 7% of the critical damping[5)], the effect of non-yielding energy dissipation is incorporated into the mathematical formulation. This simplified mathematical model and representation of the viscous damping may effect greatly on the seismic responses. In this study, a modified Rayleigh damping is used and expressed as follows

$$ {}^{t}\mathbf{C} = \alpha\mathbf{M} + \gamma\,{}^{t}\mathbf{K} + \xi\mathbf{K}_0 \qquad (2)$$

where ${}^{t}\mathbf{K}$ is the tangent stiffness matrix, $\mathbf{K}_0$ is the initial stiffness matrix, and $\alpha$, $\gamma$, and $\xi$ are proportional constants which can be evaluated from the natural frequencies of the structure.

### 2.2 Numerical Procedures

Newmark's direct integration method is used to solve the nonlinear governing equation in this study. In this method, the governing equation, Eq. (1), can be expressed as

$$ {}^{t}\mathbf{K}_{D}\ {}^{t+\Delta t}\Delta\mathbf{D}^{(k)} = {}^{t+\Delta t}\mathbf{F}_{D}^{(k)} - {}^{t+\Delta t}\mathbf{R}^{(k-1)} \qquad (3)$$

where

$$ {}^{t+\Delta t}\mathbf{F}_{D}^{(k)} = {}^{t+\Delta t}\mathbf{F}_{D}^{(k-1)} + {}^{t+\Delta t}\Delta\mathbf{F}_{D}^{(k)} \qquad (4)$$

and ${}^{t+\Delta t}\Delta\mathbf{D}^{(k)}$ is the increment of the relative displacement vector for the free degrees of freedom. ${}^{t}\mathbf{K}_{D}$ is the dynamic tangent stiffness matrix and can be shown to be

$$ {}^{t}\mathbf{K}_{D} = f_1\mathbf{M} + f_2\,{}^{t}\mathbf{K} \qquad (5)$$

${}^{t+\Delta t}\mathbf{F}_{D}^{(k-1)}$ and ${}^{t+\Delta t}\Delta\mathbf{F}_{D}^{(k)}$ are the modified external force and its incremental vector, respectively. The modified external force vector can be expressed as

$$ {}^{t+\Delta t}\mathbf{F}_D^{(k-1)} = {}^{t+\Delta t}\mathbf{F}^{(k-1)} + {}^{t+\Delta t}\mathbf{P}^{(k-1)} - \mathbf{M}\,{}^{t+\Delta t}\ddot{\mathbf{D}}_g^{(k-1)} \qquad (6) $$

and ${}^{t+\Delta t}\mathbf{R}^{(k-1)}$ is the internal force vector of the system. The term ${}^{t+\Delta t}\mathbf{P}^{(k-1)}$ in Eq. (6) is the modified force vector contributed by the displacement, velocity and acceleration at time $t$ and displacement at time $t+\Delta t$, and can be written as

$$ \begin{aligned} {}^{t+\Delta t}\mathbf{P}^{(k-1)} &= \mathbf{M}\left[f_1\,{}^t\mathbf{D} + f_3\,{}^t\dot{\mathbf{D}} + f_4\,{}^t\ddot{\mathbf{D}} - f_1\,{}^{t+\Delta t}\mathbf{D}^{(k-1)}\right] \\ &+ {}^t\mathbf{K}\left[f_5\,{}^t\mathbf{D} + f_6\,{}^t\dot{\mathbf{D}} + f_7\,{}^t\ddot{\mathbf{D}} - f_5\,{}^{t+\Delta t}\mathbf{D}^{(k-1)}\right] \end{aligned} \qquad (7) $$

The incremental external force term ${}^{t+\Delta t}\Delta\mathbf{F}_D^{(k)}$ can be shown to be

$$ {}^{t+\Delta t}\Delta\mathbf{F}_D^{(k)} = {}^{t+\Delta t}\Delta\mathbf{F}^{(k)} - \mathbf{M}\,{}^{t+\Delta t}\Delta\ddot{\mathbf{D}}_g^{(k)} \qquad (8) $$

The coefficients, $f_i$'s, are constants and can be evaluated[6] in terms of $\eta$, $\alpha$, $\beta$, $\gamma$, and $\Delta t$ as

$$ \begin{aligned} & f_1 = \frac{1}{\beta\Delta t^2} + \frac{\eta\alpha}{\beta\Delta t}, \quad f_2 = \frac{\eta\gamma}{\beta\Delta t} + 1, \quad f_3 = \frac{1}{\beta\Delta t} + \frac{\eta\alpha}{\beta} - \alpha, \\ & f_4 = \left(\frac{1}{2\beta} - 1\right) + \eta\alpha\left(\frac{1}{2\beta} - \frac{1}{\eta}\right)\Delta t, \quad f_5 = \frac{\eta\alpha}{\beta\Delta t}, \\ & f_6 = \frac{\eta\gamma}{\beta} - \gamma, \quad f_7 = \left(\frac{\eta\gamma}{2\beta} - \gamma\right)\Delta t \end{aligned} \qquad (9) $$

Eq. (3) now can be solved by the modified Newton-Raphson method. Once the displacements are obtained, the member forces can be calculated accordingly.

## 3. Uncertainties in Time-variant Dynamic and Seismic Loadings

Considering uncertainties in time-variant dynamic loading is very challenging. For the clarity of discussion, it is important to differentiate between the short and long duration loadings. For long duration loadings, the works of Bucher, Chen, and Schüller[7] and Yao and Wen[8] are noteworthy. Bucher, Chen, and Schüller[7] converted the time-variant problem to a time-invariant problem by applying the lifetime maximum effect of combined load processes after evaluating the limit state function. Bucher and Bourgund[9] and Rajashekhar and Ellingwood[10] considered short duration loadings. They examined the same dynamic problem, which is a nonlinear single degree of freedom (SDOF) oscillator with random system parameters subjected to a rectangular load pulse with random duration and amplitude. Their procedures cannot be used for the reliability analysis of nonlinear structures subjected to general short duration loadings including seismic loading.

Seismic loading is essentially a short duration loading. There is no guideline as how to consider uncertainties in both the amplitude and frequency in the seismic loading. The uncertainty in the amplitude of the earthquake is successfully considered in the context of RSM in this study, that is, the sampling points will be selected, as shown conceptually in Fig. 1, to consider uncertainties in the amplitude. The uncertainty in the frequency content of an earthquake can be considered indirectly. Avail-

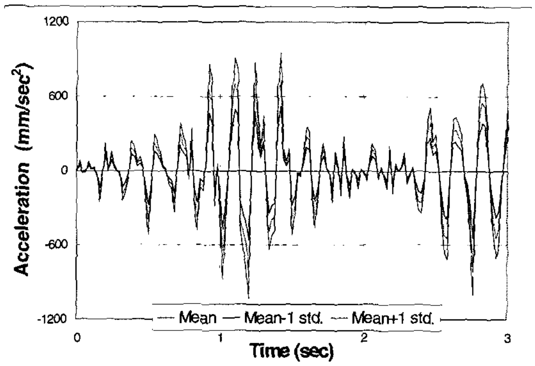


Fig. 1 Consideration of uncertainty in the amplitude of an earthquake

able time histories for an actual earthquake are first normalized with respect to the peak acceleration. Then the reliability of structures can be estimated using the algorithm developed in this study. Since all the time histories have different frequency content, the estimated reliability will indicate the effect of uncertainties in the frequency content.

## 4. A Unified Stochastic Finite Element Method

The proposed algorithm intelligently integrates the concepts of RSM, FEM, FORM, and an iterative linear interpolation scheme. First, responses are calculated at the experimental sampling points of the response surface model, that is, saturated design with the second order polynomial without cross terms, by conducting nonlinear FEM. The initial center point is assumed to be the mean values of random variables for the first iteration. A limit state function is thus generated in terms of $k$ basic random variables. Using the explicit expression for the limit state function and FORM, the reliability index $\beta$, and the corresponding coordinates of the checking point and direction cosines for each random variable are obtained.

The new center point for the next iteration is obtained by applying a linear interpolation scheme. The updating of the center point continues until it converges to a predetermined tolerance level. In the final iteration, the information on the most recent center point is used to formulate the final response surface using either saturated design with a full second order polynomial or central composite design with a full second order polynomial depending on the number of random variables. This gives an explicit expression of the limit state function.

The FORM method is then used to calculate the reliability index and the corresponding the most probable failure point (MPFP). Some of the salient features of the proposed algorithm are discussed in the following sections.

### 4.1 Response Surface Method

RSM is an important element of the proposed study. The primary purpose of applying RSM in reliability analysis is to approximate the original complex and implicit limit state function using a simple and explicit polynomial[7),9),10),11)]. Since the nonlinear time domain seismic response of structures is considered, at least a second order polynomial is necessary.

In this study, two types of second order polynomial, i.e., with and without cross terms, are used to represent the response surface. They can be expressed as

$$\hat{g}(\mathbf{X}) = b_0 + \sum_{i=1}^{k} b_i X_i + \sum_{i=1}^{k} b_{ii} X_i^2 \qquad (10)$$

$$\hat{g}(\mathbf{X}) = b_0 + \sum_{i=1}^{k} b_i X_i + \sum_{i=1}^{k} b_{ii} X_i^2 + \sum_{i=1}^{k-1} \sum_{j>i}^{k} b_{ij} X_i X_j \qquad (11)$$

where $X_i (i=1,\cdots,k)$ is the $i^{th}$ random variable, and $b_0$, $b_i$, $b_{ii}$, and $b_{ij}$ are unknown coefficients to be determined. The number of coefficients for each polynomial in Eq. (10) and Eq. (11) are $p_1=2k+1$ and $p_2=(k+1)(k+2)/2$, respectively.

The polynomials can be fully defined either by solving a set of linear equations or from regression analysis for the responses at specific data points called experimental sampling points. The selection of experimental sampling points where responses need to be calculated is known as experimental design. Saturated design and the central composite design could be the two most promising ones among the techniques available to generate sampling points.

Although the details of experimental design cannot be given here due to lack of space, they can be found in the literature[12),13)].

### 4.2 Proposed Response Surface Model and Iterative Schemes

Considering the form of the polynomial and the selection requirements for the experimental sampling points, the three response surface models suggested by Huh[14)] are considered in this paper: Model (1): Saturated deign using a second order polynomial without cross terms, Model (2): Saturated design using a full second order polynomial, and Model (3): Central composite design using a full second order polynomial.

#### 4.2.1 Model (1): Saturated Design using a Second Order Polynomial without Cross Terms

The response surface of this model is represented by Eq. (10). It consists of a center point and $2k$ star points (one at +1 and one at -1 for each variable in the coded variables space), i.e., the total number of experimental sampling points, $N=p=2k+1$, in which $k$ and $p$ are defined in the previous section. The experimental sampling points for this model in coded values are tabulated in Table 1 for $k$=3. This model requires the least experimental sampling points among three models, i.e., the least number of deterministic dynamic analyses. However, it could be less accurate than others since it does not cover sample spaces between the axes; that is, absence of $X_iX_j$ (two factor interaction) term in this model.

Table 1 Experimental sampling points of model (1) in coded values for $k$=3

| | No. | $\chi_1$ | $\chi_2$ | $\chi_3$ |
|---|---|---|---|---|
| 1 | 1 | -1 | 0 | 0 |
| 2 | 2 | +1 | 0 | 0 |
| : | 3 | 0 | -1 | 0 |
| : | 4 | 0 | +1 | 0 |
| $2k$-1 | 5 | 0 | 0 | -1 |
| $2k$ | 6 | 0 | 0 | +1 |
| $2k$+1 | 7 | 0 | 0 | 0 |

#### 4.2.2 Model (2): Saturated Design using a Full Second Order Polynomial

In this model, the polynomial expressed by Eq. (11) is used to improve the accuracy of the response surface by inclusion of the cross terms, which represent the interaction effect of two variables $X_i$ and $X_j$. This model consists of one center point, $2k$ star points, and $k(k-1)/2$ edge points, resulting the total number of experimental sampling points to be exactly as many points as the terms in the polynomial, $N=p=(k+1)(k+2)/2$. An edge point[15)] is a $k$-vector having ones in the $i^{th}$ and $j^{th}$ location and zeros elsewhere. The experimental sampling points for this model are given in Table 2 for $k$=3. This model is expected to be more accurate and less efficient than Model (1).

#### 4.2.3 Model (3) : Central Composite Design using a Full Second Order Polynomial

The response surface of this model is expressed by Eq. (11). It consists of: (a) a complete $2^k$ factorial design, where the factor levels are

Table 2 Experimental sampling points of model (2) in coded values for $k$=3

| | No. | $\chi_1$ | $\chi_2$ | $\chi_3$ |
|---|---|---|---|---|
| 1 | 1 | -1 | 0 | 0 |
| 2 | 2 | +1 | 0 | 0 |
| : | 3 | 0 | -1 | 0 |
| : | 4 | 0 | +1 | 0 |
| $2k$-1 | 5 | 0 | 0 | -1 |
| $2k$ | 6 | 0 | 0 | +1 |
| $2k$+1 | 7 | +1 | +1 | 0 |
| : | 8 | +1 | 0 | +1 |
| : | 9 | 0 | +1 | +1 |
| $(k+1)(k+2)/2$ | 10 | 0 | 0 | 0 |

Table 3 Experimental sampling points of model (3) in coded values for $k$=3

| | No. | $x_1$ | $x_2$ | $x_3$ |
|---|---|---|---|---|
| 1 | 1 | -1 | -1 | -1 |
| 2 | 2 | +1 | -1 | -1 |
| : | 3 | -1 | +1 | -1 |
| : | 4 | +1 | +1 | -1 |
| : | 5 | -1 | -1 | +1 |
| : | 6 | +1 | -1 | +1 |
| $2^k$-1 | 7 | -1 | +1 | +1 |
| $2^k$ | 8 | +1 | +1 | +1 |
| $2^k$+1 | 9 | $-\alpha$ | 0 | 0 |
| : | 10 | $+\alpha$ | 0 | 0 |
| : | 11 | 0 | $-\alpha$ | 0 |
| : | 12 | 0 | $+\alpha$ | 0 |
| : | 13 | 0 | 0 | $-\alpha$ |
| $2^k+2k$ | 14 | 0 | 0 | $+\alpha$ |
| $2^k+2k+1$ | 15 | 0 | 0 | 0 |

coded to the usual -1, +1 values, (b) one center point, and (c) two axial points on the axis of each random variable at a distance of $\alpha$ from the center point where $\alpha = \sqrt[4]{2^k}$ in order to make the design rotatable. Thus, the total number of experimental sampling points is $N=2^k+2k+1$, which are much more than the number of the coefficient $p=(k+1)(k+2)/2$. The experimental sampling points for this model are given in Table 3 for $k$=3. This model is expected to be more accurate and less computationally efficient than the two previous models, particularly when the number of random variables to be considered is large. It also contains several statistical properties, such as analysis of variance (ANOVA), orthogonality, and rotatability.

### 4.2.4 Proposed Iterative Schemes

The three models need to be intelligently integrated to achieve the computational efficiency and the accuracy of the proposed algorithm. It is observed that the efficiency and accuracy of the proposed algorithm can be increased by applying the two promising schemes.

Scheme 1. Saturated design using a second order polynomial without cross terms is used for the intermediate iterations and saturated design using a full second order polynomial is used for the final iteration when the number of random variables to be considered is large, say more than 9.

Scheme 2. Saturated design using a second order polynomial without cross terms is used for the intermediate iterations and central composite design using a full second order polynomial is used for the final iteration when the number of random variables to be considered is moderate, say less than 9.

This will be discussed further with help of an example.

Based on the proposed algorithm, a new dynamic

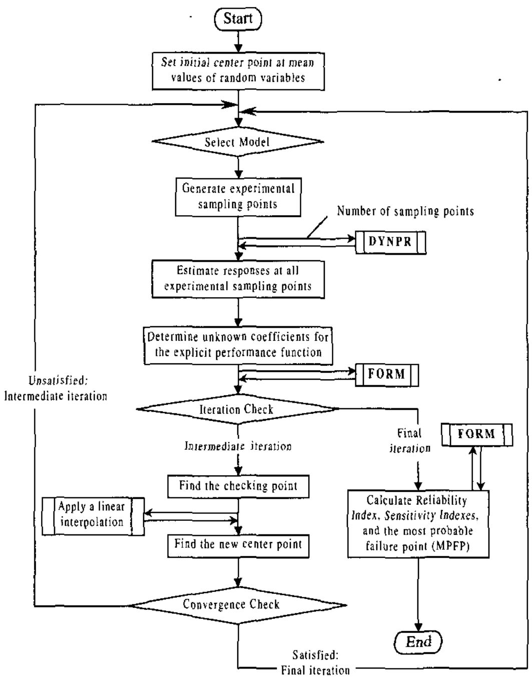

Fig. 2 Flowchart of the proposed algorithm (Program RSDRA)

reliability analysis program RSDRA is developed by combining a deterministic dynamic analysis program[1] (DYNPR) with a new reliability program. The flowchart that shows all the main steps of the proposed algorithm is given in Fig. 2.

### 4.3 Analysis of Variance

Analysis of variance (ANOVA) is used to represent measures of information about the separate sources of variation, i.e., error, for the central composite design. The coefficient of determination, $R^2$, which is a measure of the proportion of total variation of the values of the actual response about its mean explained by the fitted response model, is calculated as

$$R^2 = \frac{SSR}{SST} \tag{12}$$

where the total sum of squares (SST) and the sum of squares due to regression (SSR) can be computed as, respectively

$$SST = \mathbf{Y}^T\mathbf{Y} - \frac{(\mathbf{1}^T\mathbf{Y})^2}{N} \tag{13}$$

$$SSR = \hat{\mathbf{Y}}^T\mathbf{Y} - \frac{(\mathbf{1}^T\mathbf{Y})^2}{N} \tag{14}$$

where $\mathbf{Y}$ is a $N\times 1$ vector of actual response values, $\hat{\mathbf{Y}}$ is the $N\times 1$ vector of response values from the fitted surface, and $\mathbf{1}^T$ is a $1\times N$ vector of ones.

### 4.4 Iterative Linear Interpolation Scheme for Determination of the Center Point

It is important to locate the center point be close to the most probable failure point (MPFP) so that the response surface thus obtained includes most of the failure region, resulting an accurate reliability estimation. Bucher and Bourgund[9] and Rajashekhar and Ellingwood[10] suggested an iterative linear interpolation scheme that can be used to locate the center point efficiently and accurately in a systematic approach, as discussed below.

In the iterative scheme, the center point is initially selected to be the mean values of the random variable $X_i$'s. Then, using the values of g(X) obtained from the deterministic FEM evaluations for all the experimental sampling points, the response surface $\hat{g}_1(\mathbf{X})$ can be generated explicitly in terms of the random variable $X_i$. Once a closed form of the limit state function, $\hat{g}_1(\mathbf{X})$, is obtained, the coordinates of the checking point $\mathbf{x}_{D_1}$ can be estimated using FORM. The actual response can be evaluated again at the checking point $\mathbf{x}_{D_1}$, i.e., $g(\mathbf{x}_{D_1})$ and a new center point $\mathbf{x}_{C_2}$ can be selected using linear interpolation from the center point $\mathbf{x}_{C_1}$ to $\mathbf{x}_{D_1}$ such that $g(X)=0$; i.e.,

$$\mathbf{x}_{C_2} = \mathbf{x}_{C_1} + (\mathbf{x}_{D_1} - \mathbf{x}_{C_1})\frac{g(\mathbf{x}_{C_1})}{g(\mathbf{x}_{C_1}) - g(\mathbf{x}_{D_1})} \quad \text{if } g(\mathbf{x}_{D_1}) \geq g(\mathbf{x}_{C_1}) \tag{15}$$

$$\mathbf{x}_{C_2} = \mathbf{x}_{D_1} + (\mathbf{x}_{C_1} - \mathbf{x}_{D_1})\frac{g(\mathbf{x}_{D_1})}{g(\mathbf{x}_{D_1}) - g(\mathbf{x}_{C_1})} \quad \text{if } g(\mathbf{x}_{D_1}) < g(\mathbf{x}_{C_1}) \tag{16}$$

A new center point $\mathbf{x}_{C_2}$ then can be used to develop an explicit performance function for the next iteration. This iteration scheme is repeated until a preselected convergence criterion is satisfied.

## 5. Numerical Example

To elaborate the algorithm further and verify its accuracy and efficiency, a two-story frame shown in Fig. 3 is considered. All the beams

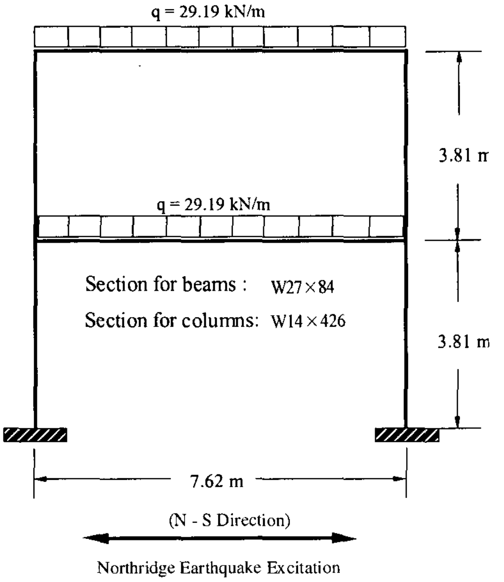

Fig. 3 Two-story steel frame structure

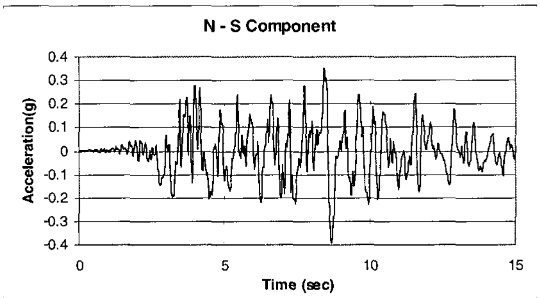

Fig. 4 Northridge earthquake time history for 15 seconds (N-S)

and columns of the frame are made of W27×84 and W14×426, respectively, and A36 steel is used for this example. The frame is excited for 15 seconds by the actual acceleration time history recorded at the Canoga Park during the Northridge earthquake of 1994 (North-South component) as shown in Fig. 4.

For the serviceability limit state, the permissible lateral displacement at the top of the frame is considered not to exceed ***h***/400, where ***h*** is the height of the frame. Of course any other value can be used for this purpose. Thus, for this example, $\delta_{allow}$ becomes 1.905cm, and the corresponding limit state can be written as

$$g(\mathbf{X}) = \delta_{allow} - y_{max}(\mathbf{X}) = 1.905 - y_{max}(\mathbf{X}) \qquad (17)$$

in which $y_{max}(\mathbf{X})$ is the maximum lateral displacement at the top of the frame.

All 9 variables shown in Table 4 are initially considered to be random. This is denoted hereafter as Case 1. From the sensitivity analysis, it was found that the sensitivity index for plastic section modulus of the beam and columns is very low compare to the others. By retaining the two variables ($Z^b_x$ and $Z^c_x$) at their mean values, only the remaining 7 variables are thus considered to be random in Case 2. For each

Table 4 Statistical description of random variablesRandom

| Random Variable | Mean Value | Case 1 | | Case 2 | |
|---|---|---|---|---|---|
| | | C.O.V. | Distribution | C.O.V. | Distribution |
| E ($kN/m^2$) | $1.9994\times10^8$ | 0.06 | Log-Normal | 0.06 | Log-Normal |
| $A^b$ ($m^2$) | $1.600\times10^{-2}$ | 0.05 | Log-Normal | 0.05 | Log-Normal |
| $I^b_x$ ($m^4$) | $1.186\times10^{-3}$ | 0.05 | Log-Normal | 0.05 | Log-Normal |
| $Z^b_x$ ($m^3$) | $3.998\times10^{-3}$ | 0.05 | Log-Normal | - | - |
| $A^c$ ($m^2$) | $8.065\times10^{-2}$ | 0.05 | Log-Normal | 0.05 | Log-Normal |
| $I^c_x$ ($m^4$) | $2.747\times10^{-3}$ | 0.05 | Log-Normal | 0.05 | Log-Normal |
| $Z^c_x$ ($m^3$) | $1.424\times10^{-2}$ | 0.05 | Log-Normal | - | - |
| $\xi$ | 0.05 | 0.15 | Log-Normal | 0.15 | Log-Normal |
| $g_e$ | 1.00 | 0.20 | Type I | 0.20 | Type I |

Table 5 Results of the reliability analysis

| Monte Carlo Simulation | | $P_f$=0.02887 ($\beta$=1.898) | | CPU Time=98183sec | |
|---|---|---|---|---|---|
| Case | | Case 1 (9 R.V.) | | Case 2 (7 R.V.) | |
| Proposed Algorithm | Scheme | Scheme 1 | Scheme 2 | Scheme 1 | Scheme 2 |
| | $P_f$ | 0.026969 | 0.028715 | 0.027450 | 0.027792 |
| | β | 1.927 | 1.900 | 1.920 | 1.914 |
| | TNSP | 93 | 569 | 66 | 173 |
| | CPU Time | 109.3sec | 567.9sec | 79.7sec | 182.8sec |
| | Error | 6.58% | 0.54% | 4.92% | 3.73% |
| Sensitivity Index $\gamma$ | E | -0.0980 | -0.2223 | -0.3931 | -0.2389 |
| | $A^b$ | 0.0151 | 0.0077 | 0.0119 | 0.0109 |
| | $I^b_x$ | -0.1195 | -0.1262 | -0.2219 | -0.1290 |
| | $Z^b_x$ | 0.0000 | 0.0001 | - | - |
| | $A^c$ | 0.0455 | 0.0201 | 0.0360 | 0.0349 |
| | $I^c_x$ | -0.1127 | -0.1190 | -0.1983 | -0.1118 |
| | $Z^c_x$ | 0.0000 | 0.0001 | - | - |
| | ξ | -0.3100 | -0.2833 | -0.2723 | -0.2792 |
| | $g_e$ | 0.9301 | 0.9164 | 0.8254 | 0.9135 |
| ANOVA | $R^2$ | N/A | 98.41% | N/A | 98.50% |
| | SST | | 10.454 | | 3.618 |
| | SSR | | 10.289 | | 3.564 |

case, all the random variables present in the formulation are given in Table 4. The term ξ is the damping coefficient expressed as a percent of the critical damping and the term $g_e$ is a parameter introduced to incorporate uncertainty in the amplitude of seismic acceleration. The statistical descriptions of most of the random variables, except the damping coefficient ξ and the amplitude of seismic acceleration $g_e$, were extensively studied in the literature[16),17)] and are given in Table 4. The damping coefficient ξ and the amplitude of seismic acceleration $g_e$ are assumed to have Type I distribution and their COV's are also assumed to be 0.15 and 0.20, respectively. All random variables are assumed to be independent for the numerical calculation.

Using the proposed nonlinear SFEM algorithm, the probability of failure of the frame for both cases is estimated. In each case, two types of schemes identified in Section 4.2.4 are considered. The results of both cases are tabulated in Table 5 in terms of probability of failure, reliability index, error, CPU time, total number of experimental sampling points (TNSP), and sensitivity indices of the random variables. For Scheme 2 of each case, the results of analysis of variance (ANOVA) such as SST, SSE, and $R^2$ values are given in Table 5 since it is only available when the central composite design is used. The results are compared with Monte Carlo simulation result using 100,000 simulations. This result is also shown in Table 5. A super computer (SGI Origin 200) was used for the numerical calculation of both proposed algorithm and Monte Carlo simulation.

It is shown in the Table 5 that the probability of failure for both cases is very close to the MCS result. In Case 1, the ratio of CPU time required for Scheme 1 and Scheme 2 of the proposed algorithm to that of MCS is found to be approximately 1/898 and 1/173, respectively.

In Case 2, they are 1/1232 and 1/537. The proposed algorithm is therefore viable and efficient for the reliability analysis of nonlinear structures subjected to seismic loadings.

Since the error of Scheme 2 is found to be less than that of Scheme 1 for both cases, the use of Scheme 2 is expected to be very accurate without sacrificing efficiency when the number of random variable considered is moderate, say less than 9. When the number of random variable, however, is large as in Case 1, the CPU time and TNSP required for Scheme 2 are very large compare to Scheme 1, making it computationally very inefficient. Thus, considering both accuracy and efficiency, Scheme 1 is recommended particularly when the number of random variables in the formulation is large; say more than 9. Of course, the number of random variables can be reduced using sensitivity analysis and then Scheme 2 can be used to obtain more accurate result. For large practical problems, therefore, the use of sensitivity analysis with Scheme 2 is expected to be very desirable. It should also be noted that in both cases when the central composite design is used; that is, Scheme 2, $R^2$ values are found to be greater than 98%. It indicates that approximately 98% of the total variation of the limit state function is explained by the fitted second order polynomial models obtained from the central composite design, resulting very low errors when Scheme 2 is used for both cases.

It was also observed that Case 2 with fewer random variables is more efficient than Case 1.

## 6. Conclusions

A relatively efficient and accurate nonlinear SFEM algorithm is proposed to estimate the reliability of structures subjected to seismic loading in the time domain. Uncertainties in the seismic excitation and resistance-related parameters are incorporated. A realistic representation of the loading conditions is considered by using actual earthquake loading time-histories to excite structures. The proposed algorithm intelligently integrates the concepts of the finite element method, the response surface method, the first order reliability method, and the iterative linear interpolation scheme. With the help of an example, it is proved that the proposed algorithm can be used to estimate the risk for nonlinear structures subjected to short duration dynamic loadings, including seismic loading. The iterative schemes suggested to improve the computational efficiency of the RSM appears to be effective. For large practical problems, the use of sensitivity analysis with Scheme 2, i.e., saturated design using a second order polynomial without cross terms for the intermediated iterations and central composite design using a full second order polynomial for the final iteration, is expected to be very desirable.

## References


1. Haldar, A. and Gao, L., Reliability evaluation of structures using nonlinear SFEM, *Uncertainty Modeling in Finite Element, Fatigue, and Stability of Systems*, edited by A. Haldar, A. Guran, and B.M. Ayyub, World Scientific Publishing Co., 1997, pp.23~50
2. Kondon, K., and Atluri, S. N., "Large-deformation, elasto-plastic analysis of frames under nonconservative loading, using explicitly derived tangent stiffnesses based on assumed stresses", *Computational Mechanics*, Vol. 2, No. 1, 1987, pp.1~25
3. Shi, G. and Atluri, S. N., "Elasto-plastic large deformation analysis of space frames", *Int. J. for Num. Methods in Eng.*, Vol. 26, 1988, pp.589~615.
4. Haldar, A, and Nee, K. M., "Elasto-Plastic Large

Deformation Analysis of PR Steel Frames for LRFD", *Computers and Structures*, Vol. 31, No. 5, 1989, pp.811~823

5. Leger, P. and Dussault, S., "Seismic-energy dissipation in MDOF structures", *Journal of Structural Engineering, ASCE*, Vol. 118, No. 5, 1992, pp.1251~1269
6. Nee, K. M. and Haldar, A., "The Elasto-Plastic Nonlinear Seismic Analysis of Partially Restrained Space Structures by the Assumed Stress Method", Report No. CEEM-89-104, Dept. of Civil Eng. and Engineering Mechanics, The University of Arizona, Tucson, Arizona, 1989
7. Bucher, C. G., Chen, Y. M., and Schüller, G.I., Time variant reliability analysis utilizing response surface approach, *Reliability and Optimization of Structural Systems '88: Proc., 2nd IFIP WG7.5 Conf.*, Springer-Verlag, Berlin, Germany, 1989, pp.1~14
8. Yao, T. H.-J. and Wen, Y. K., "Response surface method for time-variant reliability analysis", *Journal of Structural Engineering, ASCE*, Vol. 122, No. 2, 1996, pp.193~201
9. Bucher, C.G. and Bourgund, U., "A fast and efficient response surface approach for structural reliability problems", *Structural Safety*, .Vol. 7, 1990, pp.57~66
10. Rajashekhar, M.R. and Ellingwood, B. R., "A new look at the response surface approach for reliability analysis", *Structural Safety*, Vol. 12, 1993, pp.205~220
11. Kim, S. H. and Na, S. W., "Response surface method using vector projected sampling points", *Structural Safety*, Vol. 19, No. 1, 1997, pp.3~19
12. Box, G. P., William G. H. and Hunter, J. S., *Statistics for Experimenters: An Introduction to Design, Data Analysis and Modeling Building*, John Wiley & Sons, New York, N.Y., 1978.
13. Khuri, A. I. and Cornell, J. A., *Response Surfaces Designs and Analyses*, Marcel Dekker, New York, N.Y., 1996
14. Huh, J. "Dynamic Reliability Analysis for Nonlinear Structures Using Stochastic Finite Element Method", Ph.D. Dissertation, Dept. Of Civil Engineering and Engineering Mechanics, The University of Arizona, 1999.
15. Lucas, J. M., "Optimum Composite Designs", *Technometrics*, Vol. 16, No. 4, 1974, pp.561~567
16. Ellingwood, B., Galambos, T. V., MacGregor, J. G., and Cornell, C. A., "Development of a probability based load criterion for American national standard A58: Building code requirements for minimum design loads in buildings and other structures." Special Publication 577, National Bureau of Standards, Washington, D.C., 1980
17. Mahadevan. S. and Haldar, A., "Stochastic FEM-based Validation of LRFD", *Journal of Structural Engineering*, ASCE, Vol. 117, No. 5, 1991, pp. 1393~1412.

(접수일자 : 2000. 6. 20)